



# The effect of functionalized hydroxyapatite on the thermal degradation behaviour and flammability of polyoxymethylene copolymer

Klaudia Król-Morkisz<sup>1</sup> · Łukasz Byczyński<sup>2</sup> · Tomasz M. Majka<sup>3</sup> · Krzysztof Pielichowski<sup>3</sup> · Kinga Pielichowska<sup>1</sup> 

Received: 17 December 2021 / Accepted: 4 September 2022 / Published online: 1 October 2022  
© The Author(s) 2022

## Abstract

In this work, the effect of functionalized hydroxyapatite (HAp-g-PEG) on the thermal degradation behaviour and flammability of polyoxymethylene copolymer (POM\_C) was investigated. Organic–inorganic hybrid additive, obtained by grafting of poly(ethylene glycol) on HAp surface using 1,6-hexamethylene diisocyanate as a linker, has been incorporated into POM matrix through an extrusion process. TG analyses show that the incorporation of HAp-g-PEG into POM\_C leads to the significant improvement in the thermal stability of the polymer matrix. This is an important finding as POM, being an engineering polymer, suffers from a relatively low thermal stability that limits processing options to develop advanced composite materials. Based on TG results kinetic parameters of the thermal degradation process using Friedman isoconversional method and nonlinear regression method have been calculated; an increase in activation energy of POM degradation process after incorporation of HAp-g-PEG has been found. Thermoanalytical analyses (TG-FTIR/MS) show that incorporation of HAp-g-PEG has no significant effect on the composition of the thermal degradation products. Flammability investigations showed small effect of HAp-g-PEG 600 on the burning time and rate, however, there was a significant reduction in the amount of dripping during the material's burning process.

**Keywords** Polyoxymethylene copolymer · Functionalized hydroxyapatite · Thermal stability · Thermal degradation · Flammability

## Introduction

Acetal copolymer plastics are a group of thermoplastics that are products of polymerization of aldehydes, most often formaldehyde, with cyclic ethers. The best known and most frequently used representative of this group is polyoxymethylene (POM). Among other plastics, these materials are distinguished by better performance properties, including high mechanical strength, stiffness, hardness, resistance to

abrasive wear, low water absorption, good chemical resistance and ease of processing. POM owes these features to the high degree of ordering of the polymer chains, which is possible due to their simple, regular and linear structure [1–3]. The most important problem, especially during the processing of acetal plastics, is their poor resistance to high temperatures. POM is processed by melt processing methods dedicated to thermoplastics, such as extrusion, injection or hot pressing. Even at its melting point, when exposed to elevated temperature for too long, POM is easily depolymerized with the release of formaldehyde. The selection of appropriate POM processing conditions is a key issue in maintaining the required performance properties of the finished elements. Minor overheating of POM leads to thermal degradation, and the released formaldehyde in the presence of oxygen is transformed to formic acid that causes acidolysis and further autocatalytic breakdown of macrochains [4–6]. Archodoulaki et al. [7, 8] studied POM thermal degradation behaviour and found that the initiation mechanism of degradation of POM is random scission of the main

✉ Kinga Pielichowska  
kingapie@agh.edu.pl

<sup>1</sup> Faculty of Materials Science and Ceramics, Department of Biomaterials and Composites, AGH University of Science and Technology, al. Mickiewicza 30, 30-059 Kraków, Poland

<sup>2</sup> Faculty of Chemistry, Rzeszow University of Technology, Al. Powstańców Warszawy 6, 35-959 Rzeszów, Poland

<sup>3</sup> Department of Chemistry and Technology of Polymers, Cracow University of Technology, ul. Warszawska 24, 31-155 Kraków, Poland

chain. Moreover, the degradation initiation takes place in the amorphous regions, which undergo degradation more rapidly. Using TG-MS the major degradation product were identified—during POM degradation mainly formaldehyde is released, but in a much smaller amounts carbon dioxide and fragments from formic acid, trioxane and methoxy oligomers were also found [9]. The methyl-oxygen bonds are weak and easy to break under heat and oxygen conditions, and the continuous deformaldehyde reaction occurs. The rate of the oxidation is determined by the free radicals presence. To avoid the POM oxidation and decomposition, free radicals should be captured by antioxidants. As antioxidants for POM thermostabilization arylamines or phenols are widely applied [10, 11]. Hu and Ye [12] investigated polyamide incorporation effect on the POM thermal stability, and the obtained results demonstrated remarkable thermal stabilization effect. Sun et al. [13] investigated thermostabilization of POM via amine treatment; it was postulated that amines can deactivate Lewis acid derived from the residual initiator and formic acid formed in situ by oxidation of formaldehyde. [13]. In the next work polyethylene wax (OPE), low molecular weight polyamide 6 (LMWPA6) and triphenyl phosphate (TPP) were tested as efficient POM thermal stabilizers [14].

POM, like all polymer materials, during combustion, produces a number of gaseous products, mainly formaldehyde, 1,3,5-trioxane, water, carbon dioxide, carbon monoxide and others [1, 15]. The ignition temperature of POM is approx. 320–340 °C, while at a temperature of approx. 375 °C the material self-ignites [16]. Among all polymer materials, POM has the lowest oxygen index of 15%, which makes it a highly flammable material [17]. Low flash point and very low LOI result from the chemical structure of POM, which contains a large amount of oxygen atoms in the main chains (for POM homopolymer—53% by mass), which reduces the thermal stability of the polymer and increases its flammability.

According to the UL 94 standard, POM has the highest HB flammability class. This means that in the Horizontal Burning (HB) test, POM burns slowly, at a rate below 75 mm min<sup>-1</sup> (for POM homopolymer it is about 29.7 mm min<sup>-1</sup>). The combustion of POM in the HB test is accompanied by a drop of burned polymer drops, and a tang of formaldehyde is noticeable [18].

As shown in previous studies, the inorganic phase, which is hydroxyapatite (HAp), significantly reduces the thermal stability of POM, which in turn precludes the introduction of HAp in more than 3% by mass which can be considered as a disadvantage for application of POM/HAp composites in biomedical field [19]. A solution to this problem may be to block the hydroxyl groups on the HAp surface by attaching poly(ethylene glycol) (PEG) to them using a diisocyanate linker. The inorganic–organic hybrid system obtained in this way can be introduced into the POM matrix

by melt processing. Studies have also shown that a significant improvement in chemical stability is observed when functionalised HAp is incorporated into POM [20].

This paper presents results of the detailed research on the thermal degradation, including analysis of the volatile products, and flammability of POM in the presence of functionalized HAp. This kind of knowledge is of primary importance for (i) design of efficient POM processing routes, and (ii) development of thermal recycling protocols after polyoxymethylene-based composites' lifetime.

## Experimental

### Materials

A commercially available polyoxymethylene copolymer (POM\_C, Ultraform®, BASF) with melt flow index (MFR) 2,6 g 10 min<sup>-1</sup> was used as the matrix of the polyacetal composites. Stoichiometric HAp (Ca<sub>10</sub>(PO<sub>4</sub>)<sub>6</sub>OH<sub>2</sub>) in the form of a nanopowder with a spherical nanoparticle shape and size 99% < 100 nm, was produced by the nGimat company (USA).

1,6-hexamethylene diisocyanate (HDI) and PEG with three different mass average molecular weights: 600, 2000 and 6000 were used to modify HAp, all supplied by Sigma Aldrich. The catalyst, dibutyltin dilaurate (DBTL), was also manufactured by Sigma Aldrich. Dehydrated N, N-dimethylformamide (DMF) and ethyl alcohol were Avantor products.

Before starting the functionalization process, HAp was dried at 110 °C for 2 h. PEG was dried at 90 °C under vacuum for 2 h, as well. Functionalized HAp (HAp-g-PEG) and POM/HAp-g-PEG composites were prepared as described in Ref. [20]. Briefly, in the first step, catalyst and 1,6-hexamethylene diisocyanate were added to the HAp dispersion in dry DMF. The reaction mixture was heated up to 80 °C and stirred under dry nitrogen for two hours. Next, it was cooled down to 40 °C and solution of PEG in DMF was added, and again mixture was heated up to 60 °C and stirred for 1.5 h. After reaction, the functionalized HAp was separated from the mixture using centrifuge, washed with dry ethanol and dried.

### Methods

Thermogravimetric analysis (TGA) was performed using a TGA 550 Discovery (TA Instruments) thermogravimetric analyser, operating in dynamic mode at heating rates of 2.5, 5, 7, 10 K min<sup>-1</sup>. Samples of about 10 mg were placed in platinum crucibles, and the measurement was performed under nitrogen or air atmosphere (flow 25 mL min<sup>-1</sup>). On the basis of the obtained TG profiles, the temperatures corresponding to the mass losses were determined, respectively:

1, 3, 5, 10, 20 and 50%, which were denoted as  $T_{x\%}$ , where  $x$  was the percentage mass loss. Moreover, the first derivative of the TG curve, denoted as DTG, and the temperature corresponding to the maximum rate of mass loss ( $T_{DTGmax}$ ) was determined. In addition, the amount of solid residue was recorded in (%) at 550 °C.

The kinetics of the composites' degradation process was calculated on the basis of the data from TG measurements using isoconversional Friedman method and multiple non-linear regression method.

Analysis of the volatile decomposition products was performed with the use of the TG/FTIR/MS method. TG analysis was performed using a Mettler Toledo TGA/DSC1 apparatus. The tests were carried out in the temperature range from 25 to 500 °C, with the heating rate of 10 °C min<sup>-1</sup>. Samples of about 10 mg were placed in open alumina crucibles with a volume of 150 µl. The measurements were carried out under nitrogen atmosphere using a gas flow of 50 mL min<sup>-1</sup>. A Mettler Toledo TGA/DSC1 instrument was coupled to a Nicolet iZ10 FTIR spectrometer (Thermo Scientific), with a transfer line heated to 220 °C. Volatiles' spectra were recorded in the range from 400 to 4000 cm<sup>-1</sup> with a resolution of 4 cm<sup>-1</sup>. At the same time, the generated gases were transported by means of a quartz capillary heated to 200 °C to the ThermoStar™ mass spectrometer (Pfeiffer Vacuum), where  $m/z$  signals up to 200  $m/z$  were recorded.

The combustion properties of the samples were measured using a PCFC microcalorimeter (Testing Technology Ltd) in an oxygen atmosphere. Samples weighing about 5 mg were used, which were heated with a rate of 1 K min<sup>-1</sup> to a temperature of 750 °C. The vertical burning test of POM composites was performed according to the UL 94 horizontal flammability test (ISO 1210) for plastics. The sample length was 127 mm, width 12.7 mm, thickness was not more than 12.7 mm. The sample was marked with lines at a distance of 25 mm and 100 mm and fixed on one side in a horizontal position, and the torch was tilted relative to the sample by 45°. The burner was adjusted to give a blue flame up to 25 mm high. The exposure to the flame shall be 30 s, and if the sample burns to the 25 mm mark within these 30 s, the flame must be removed immediately. The test was performed on three samples. Based on the conducted flammability tests, the total burning time and rate of samples were determined. The flame colour, the number of droplets falling during combustion, the formation of charcoal and the ignition of the filter paper were assessed. The tests were carried out on five samples from each series. The effect of HAp-g-PEG addition on the LOI of composites in accordance with DIN EN ISO 4589-2 was also investigated using the Oxygen Index Module (Concept Fire Testing) apparatus. The oxygen content in the combustion atmosphere was determined with an accuracy of 0.1%, and the gas flow

(mixture of nitrogen and oxygen) was 10 L min<sup>-1</sup>. The specimen size was 100 × 10 × 3 mm.

The microstructure of the char residue was studied using a FEI Nova Nano SEM 200 scanning electron microscope (SEM). Samples were coated with a carbon layer just before the measurement.

## Results and discussion

As shown in previous studies, the addition of HAp-g-PEG caused a significant increase in the thermal stability of POM [21]. The obtained results revealed that during functionalization, HAp nanoparticles agglomerate in clusters probably as a result of chemical bonding by organic coupling agents—diisocyanate and PEG. Good dispersion of HAp-g-PEG clusters in POM matrix after melt processing was also observed [20].

Results of TG analysis for POM modified with HAp-g-PEG obtained at heating rate of 5 K min<sup>-1</sup>, both in inert and oxidative atmosphere are presented in Table 1.

It can be observed that a higher thermal stability increase was found for composites modified with 1% HAp-g-PEG. Depending on the additive used, the thermal stability of the material for HAp-g-PEG 600 increased from 16 °C for the POM\_C/1.0% HAp-g-PEG 2000 composite, to 24 °C for the POM\_C/1% HAp-g-PEG 6000. Moreover, in the materials containing HAp-g-PEG 600, there was a significant shift in the  $T_{DTGmax}$  temperature corresponding to the maximum degradation rate by as much as 17 °C for POM\_C/10.0% HAp-g-PEG 600.

The most effective thermal stabilizer for POM\_C turned out to be HAp-g-PEG 600, where PEG with the lowest average molar mass (PEG 600) was used for synthesis. This effect may be related to the highest mobility of this glycol and the lowest viscosity of the reaction mixture, which facilitates the grafting reaction. Thus, more hydroxyl groups reacted with isocyanate groups from diisocyanate. That reduced the number of free -OH groups in HAp, which were the basic active centers of the POM depolymerization process in POM/HAp nanocomposites [22]. The increase in the thermal stability of POM\_C may also be due to nitrogen atoms (up to 2 mass% in HAp-g-PEG 600) present in the HAp-g-PEG urethane bonds. As it is commonly known, nitrogen-containing compounds, i.e. hydrazines, aromatic amines, urea, etc., are used as POM thermal stabilizers [6]. In order to analyse more precisely the influence of HAp-g-PEG addition on POM\_C degradation, in the further part of the work, the kinetics of degradation of selected POM\_C/HAp-g-PEG composites was studied.

Both for inert and oxidative atmosphere, an increase in the thermal stability of POM has been observed after incorporation of HAp-g-PEG. However, higher enhancement

**Table 1** Thermal stability of POM\_C/HAp-g-PEG composites at heating rate of 5 K min<sup>-1</sup> in inert and oxidative atmosphere

Material	$T_{1\%}/^{\circ}\text{C}$	$T_{3\%}/^{\circ}\text{C}$	$T_{5\%}/^{\circ}\text{C}$	$T_{10\%}/^{\circ}\text{C}$	$T_{50\%}/^{\circ}\text{C}$	$T_{\text{DTG}}/^{\circ}\text{C}$
Non-oxidative atmosphere						
POM_C	289	309	319	334	375	382
POM_C/1.0% HAp-g-PEG 600	308	333	341	351	381	381
POM_C/10.0% HAp-g-PEG 600	281	334	348	360	388	399
POM_C/1.0% HAp-g-PEG 2000	305	330	339	349	381	392
POM_C/10.0% HAp-g-PEG 2000	256	322	341	353	383	395
POM_C/1.0% HAp-g-PEG 6000	313	333	340	348	379	380
POM_C/10.0% HAp-g-PEG 6000	281	333	345	356	387	395
Oxidative atmosphere						
POM_C	256	267	271	277	296	298
POM_C/1.0% HAp-g-PEG 600	269	280	283	288	305	307
POM_C/10.0% HAp-g-PEG 600	266	297	298	305	322	327
POM_C/1.0% HAp-g-PEG 2000	267	278	282	288	301	300
POM_C/10.0% HAp-g-PEG 2000	259	284	290	298	320	321
POM_C/1.0% HAp-g-PEG 6000	267	277	280	285	299	301
POM_C/10.0% HAp-g-PEG 6000	268	291	295	302	317	322

has been found during measurements in inert atmosphere. Hence, selected samples of POM\_C and POM\_C composites with HAp-g-PEG were subjected to detailed thermogravimetric analysis under inert gas atmosphere by heating them at four selected heating rates (2, 5; 5; 7 and 10 K min<sup>-1</sup>), and then the kinetic parameters of the degradation process were calculated in order to determine the influence of HAp-g-PEG incorporation on the rate of composites' thermal degradation processes. TG and DTG curves at the four heating rates for modified POM materials are presented in Fig. 1.

For all tested materials, with the increase in the heating rate, the decomposition process shifts towards higher temperatures. The shape of the TG curves suggests a one-stage degradation of all tested materials. The changing shape of the TG curves with the increase of HAp-g-PEG content indicates a change in the degradation mechanism of the tested materials. Analysis of DTG profiles shows that for composites containing 10.0% of the additive, an overlapping of at least two peaks occurs during decomposition, which indicates a complex degradation behaviour.

Calculation of the (apparent) activation energy of the POM\_C/HAp-g-PEG degradation process was performed using the Friedman method. A graphic representation of the results of Friedman's analysis is summarized in Fig. 2.

The activation energy values of the degradation process vs fractional mass loss were determined—Fig. 3.

For unmodified POM\_C, the Friedman plot shows only one maximum for each of the heating rates, indicating a one-step material decomposition. Moreover, in the first stage of the reaction, the isoconversional lines present in the graph have a greater slope than the obtained experimental points, which may indicate the autocatalytic nature of the POM\_C degradation process. This is consistent with the information

presented in the literature on the thermal degradation process of POM chains [23]. The addition of 1.0% HAp-g-PEG causes flattening and stretching of the Friedman plots of the tested composites, which may indicate the occurrence of more parallel decomposition reactions. Moreover, the activation energy diagram (for samples containing 1.0% HAp-g-PEG 600 and 2000) shows a significant increase in the value of this energy for the first 10% mass loss of the material. This effect is most likely due to improvement of the thermal stability of POM\_C in the tested composites. The Friedman plots for samples containing 10.0% HAp-g-PEG addition are characterized by the presence of two overlapping peaks, indicating that at least two consecutive decomposition reactions occur, and it can also be seen in the activation energy vs mass loss diagram.

On the basis of the TG curves obtained at four different heating rates, the form of the function  $f(\alpha)$  was determined using the non-linear regression method. For the interpretation of the results, data obtained experimentally were used, to which an appropriate model or the relationship of several models of the kinetic model function was then fitted. The degree of conversion  $\alpha$  is determined from the equation:

$$\frac{d\alpha}{dt} = f(\alpha)k(T)g(\alpha, T)q(p) \quad (1)$$

$$\alpha = \frac{\int_0^{t_1} [D(t) - B(t)]dt}{\int_0^{\infty} [D(t) - B(t)]dt} \quad (2)$$

where  $\alpha$ —degree of conversion,  $D(t)$ —measurement signal,  $B(t)$ —baseline.

In Table 2 selected physico-chemical models that are applied in solid state chemistry, kinetic considerations are

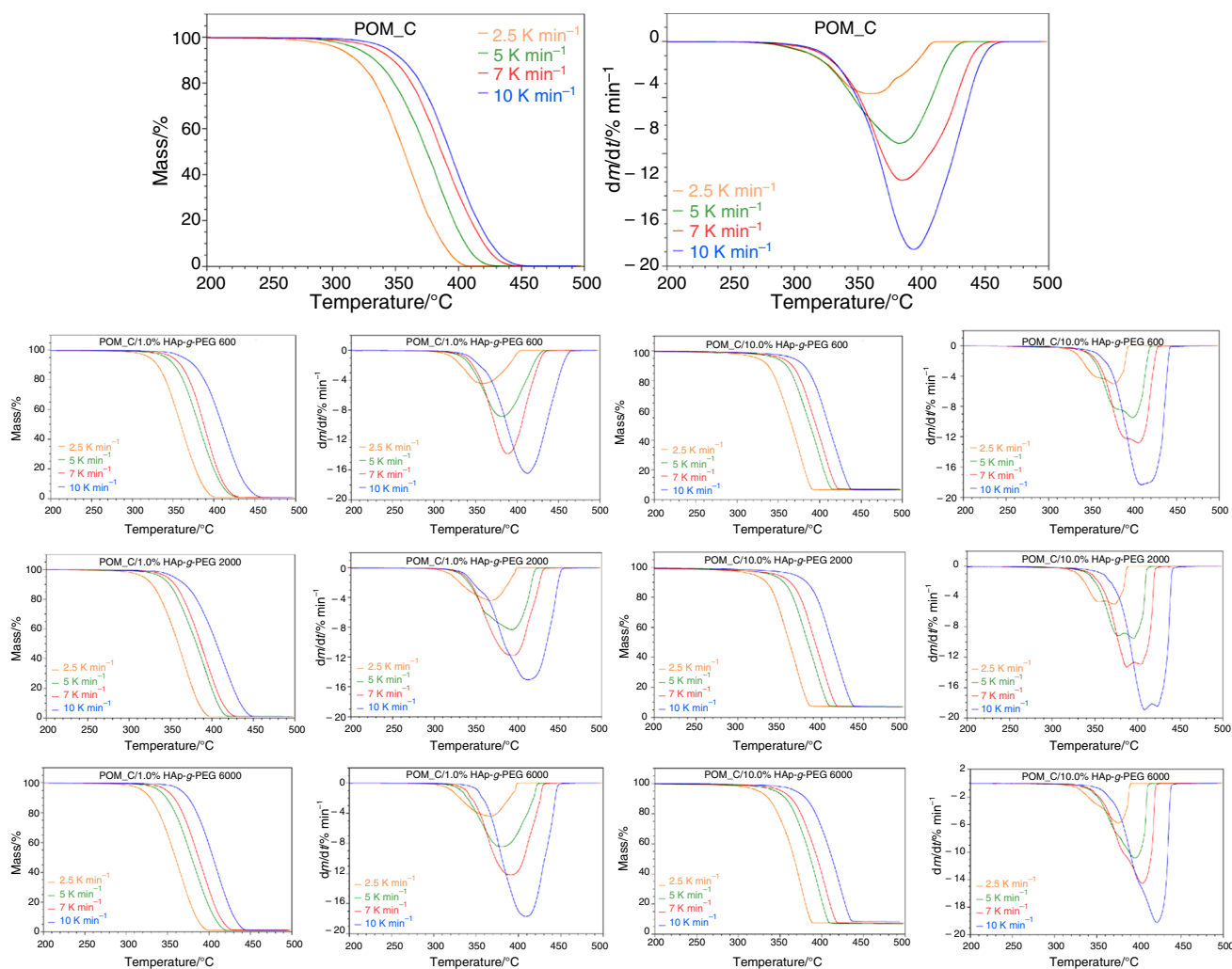


**Fig. 1** TG and DTG curves for POM\_C, POM\_C/HAp-g-PEG composites obtained at different heating rates: 2.5 K min<sup>-1</sup>, 5 K min<sup>-1</sup>, 7 K min<sup>-1</sup> and 10 K min<sup>-1</sup>

presented. In the case of polymers with a simple chain structure like for POM, thermal decomposition takes place in one step through one type of chemical reaction. As a result, it is possible to describe the decomposition process with one mathematical model. More often, in more complex polymers and composite materials, thermal decomposition is a consequence of several chemical reactions that can take place in parallel or successive. Hence, in order to describe more complex systems, it is necessary to find the relationships being combination of several mathematical models that will allow for the best adjustment with the experimental data from TG measurements.

The results of mathematical fit of different model functions to the thermal decomposition pathway of POM\_C and its composites are showed in Fig. 4 and Table 3.

The degree of matching of the models to the measurement data was determined by using the 'F-test' statistical test. For unmodified POM\_C, the best fit is the one-step

Prout-Tompkins reaction model with an autocatalysis (Bna). It is a reaction accompanied by the release of gaseous products (for POM → formaldehyde), which has a catalytic effect on the further course of the reaction, significantly accelerating this process [25]. This result is in line with previous studies for POM copolymer [22, 25]. For pristine POM\_C, the activation energy of the reaction is about 117.5 kJ mol<sup>-1</sup>. The thermal decomposition of POM\_C is a first-order reaction, which is consistent with the literature data [26]. For composites containing 1.0% HAp-g-PEG additive, material decomposition is a more complex process, consisting of two parallel degradation reactions. Autocatalytic reactions (Bna, Cn) still play a dominant role, but at the same time, there is *n*-dimensional nuclei growth following the Avrami equation (An). In composites with a high additive content (POM\_C/10.0% HAp-g-PEG), thermal decomposition takes place in several stages as a result of subsequent reactions. The best fit of the models for the systems with

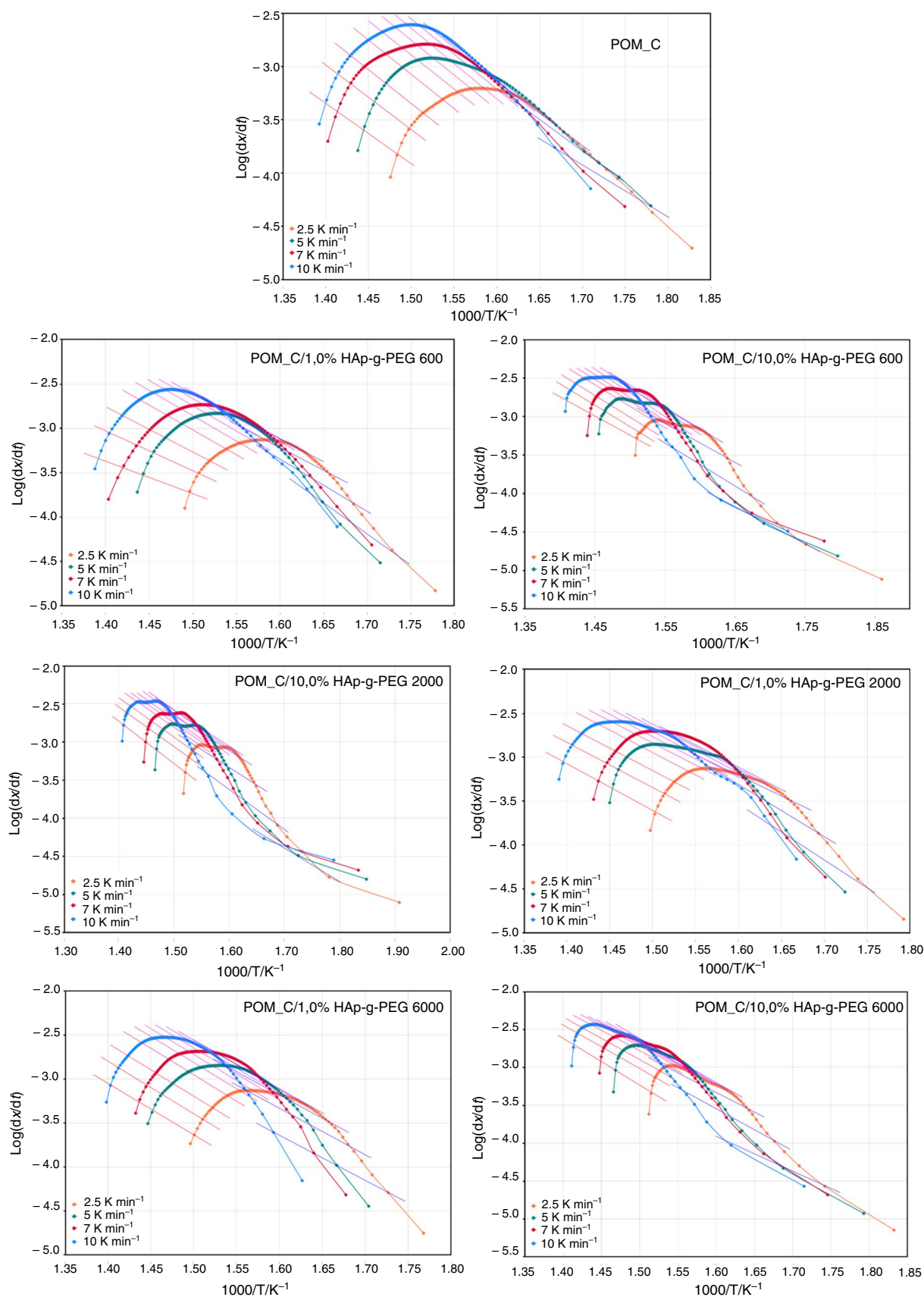


**Fig. 2** The results of the Friedman analysis of the POM\_C thermal decomposition process and POM\_C composites with 1.0% and 10.0% HAp-g-PEG

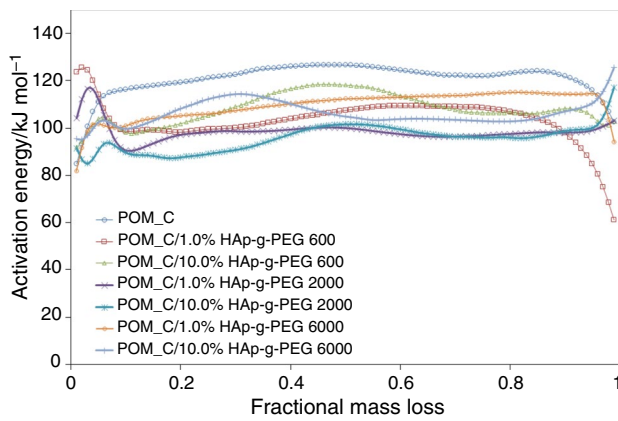


**Fig. 3** The activation energy values determined from the Friedman analysis of the POM\_C thermal decomposition process and POM\_C composites with 1.0% and 10.0% HAp-g-PEG

the addition of HAp-g-PEG 600 and HAp-g-PEG 2000 is the  $n$ -dimensional nuclei growth followed by the  $n$ -th order reaction without a pronounced autocatalysis. An equally well-fitted decomposition model shows in the first decomposition stages the dominant influence of the  $n$ th-order reaction with an accompanying autocatalytic effect (Bna, Cn), which is preceded by the  $n$ -dimensional nuclei growth (An) at the lowest temperatures. At the end of the thermal decomposition, interfacial reactions related to the presence of a large amount of HAp-g-PEG addition are observed. When the PEG average molar mass in HAp-g-PEG systems is lower, a phase boundary-controlled reaction (contracting area) (R2) is observed, for a higher molecular weight of PEG it is a phase boundary-controlled reaction (contracting

volume) (R3). As a consequence, the thermal decomposition of POM is slowed down and the mass loss shifted towards higher temperatures. Thanks to this, it is possible to run melt processing of these POM-based materials, reducing their risk of degradation during processing.

TG-FTIR/MS hyphenated technique was used to perform an in-depth investigation of the thermal decomposition of polyoxymethylene composites containing 1.0% and 5.0% HAp-g-PEG. The results of TG-FTIR in the form of three-dimensional graphs (stacked plots) of all measured FTIR spectra of volatile decomposition products evolved in the temperature range from 25 to 550 °C are shown in Fig. 5.

From the presented results, no decomposition products can be observed during the first 30 min of heating up to about 325 °C. The decomposition of the materials takes place between 30 and 45 min, which corresponds to temperature range of 325–475 °C. The results show a shift in the onset of thermal decomposition toward higher temperatures for composite materials, which confirms their increased thermal stability compared to non-modified POM\_C. For each of the composite under investigation, five individual spectra were selected to show changes in the characteristic absorption bands—Fig. 6.

For unmodified POM\_C, the most intense decomposition occurred at ca. 365 °C, while for composite materials this temperature was higher, up to 8 and 10 °C for POM containing 1.0% and 5.0% of HAp-g-PEG 600, respectively. For other compositions, the increase in the temperature of decomposition was shifted from 5 to 7 °C; these results stay in good agreement with TG results.

The following absorption bands are visible in POM\_C thermal decomposition spectra: 1027  $\text{cm}^{-1}$  from the carbonyl

**Table 2** Selected kinetic model functions  $f(\alpha)$  [24]

Reaction model	Function $f(\alpha)$	Symbol
First-order reaction	$(1 - \alpha)$	F1
Second order reaction	$(1 - \alpha)^2$	F2
$n$ -th order reaction	$(1 - \alpha)^n$	Fn
One-dimensional diffusion	$1/2\alpha$	D1
Two-dimensional diffusion	$1/[-\ln(1 - \alpha)]$	D2
Three-dimensional diffusion, Jander equation	$3(1 - \alpha)^{2/3}/2[1 - (1 - \alpha)^{1/3}]$	D3
Three-dimensional diffusion, Ginstling-Brounshtein equation	$3/2[(1 - \alpha)^{-1/3} - 1]$	D4
Phase boundary-controlled reaction (contracting area)	$(1 - \alpha)^{1/2}$	R2
Phase boundary-controlled reaction (contracting volume)	$(1 - \alpha)^{2/3}$	R3
Autocatalytic reaction, Prout-Tompkins equation	$(1 - \alpha)\alpha$	B1
$A$ -th degree autocatalytic reaction with $n$ -order reaction, Prout-Tompkins equation	$(1 - \alpha)^n \alpha^a$	Bna
First order reaction with autocatalytic effect	$(1 - \alpha)(1 + J_{\text{kat}}\alpha)$	C1
$N$ -th order reaction with autocatalytic effect	$(1 - \alpha)^n(1 + J_{\text{kat}}\alpha)$	Cn
Two-dimensional nuclei growth, Avrami-Erofeev equation	$2[-\ln(1 - \alpha)^{1/2}](1 - \alpha)$	A2
Three-dimensional nuclei growth, Avrami-Erofeev equation	$3[-\ln(1 - \alpha)^{2/3}](1 - \alpha)$	A3
$N$ -dimensional nuclei growth, Avrami-Erofeev equation	$n[-\ln(1 - \alpha)^n](1 - \alpha)$	An

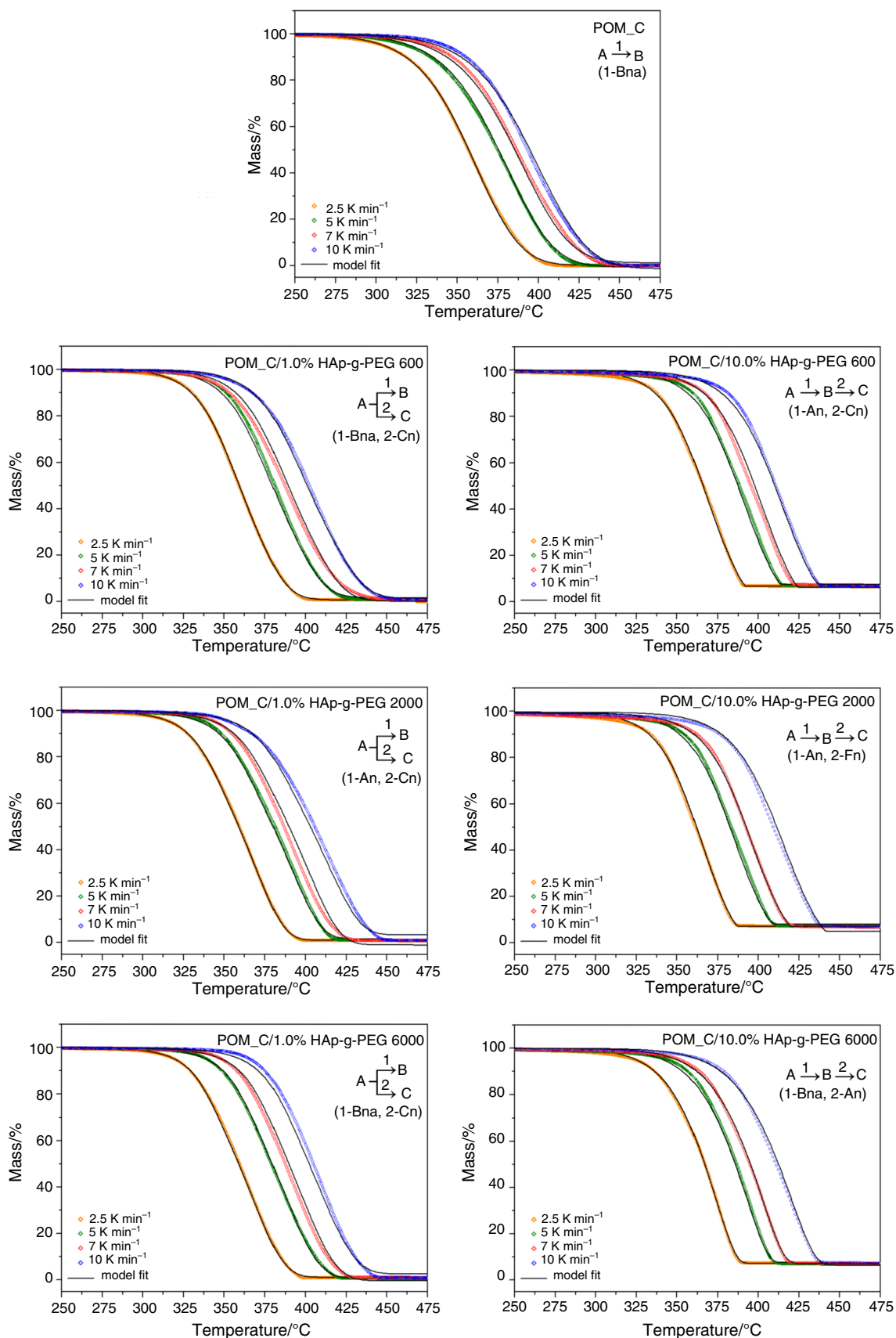


**Fig. 4** Best fits of kinetic models to the thermal degradation profiles of POM\_C and its composites with 1.0% and 10.0% HAp-g-PEG 600, HAp-g-PEG 2000 and HAp-g-PEG 6000



**Table 3** The results of mathematical fitting of kinetic model functions to the thermal decomposition profiles of POM\_C and POM/ HAp-g-PEG composites

Material	Stage I				Stage II				Stage III				F-test			
	$E_{a1}$ , kJ mol <sup>-1</sup>	logA <sub>1</sub>	Reaction order	Dimension	Model	$E_{a2}$ , kJ mol <sup>-1</sup>	logA <sub>2</sub>	Reaction order	Dimension	Model	$E_{a3}$ , kJ mol <sup>-1</sup>	logA <sub>3</sub>		Reaction order	Dimension	Model
POM_C	117.54	6.95	1.12	-	Bna	-	-	-	-	-	-	-	-	-	-	1.00
	118.47	6.89	-	1.13	An	-	-	-	-	-	-	-	-	-	-	1.38
	117.48	6.64	1.35	-	Cn	-	-	-	-	-	-	-	-	-	-	1.47
POM_C/1.0% HAp-g-PEG 600	110.27	6.67	1.10	-	Bna	104.73	4.72	1.07	-	Cn	-	-	-	-	-	1.00
	107.37	6.33	1.05	-	Bna	113.25	6.23	-	1.62	An	-	-	-	-	-	1.10
	108.70	6.35	1.13	-	Bna	-	-	-	-	-	-	-	-	-	-	1.15
POM_C/10.0% HAp-g-PEG 600	101.81	5.50	-	2.07	An	117.09	6.60	0.28	-	Fn	-	-	-	-	-	1.07
	105.53	5.18	0.73	-	Cn	119.04	6.41	-	4.62	An	138.94	8.42	-	-	R2	1.10
	102.86	5.97	0.60	-	Bna	119.89	6.43	-	5.21	An	154.70	9.76	-	-	R2	1.13
POM_C/1.0% HAp-g-PEG 2000	105.14	5.64	-	2.03	An	104.04	5.19	1.46	-	Cn	-	-	-	-	-	1.00
	100.97	5.79	1.11	-	Bna	111.37	6.14	-	1.88	An	-	-	-	-	-	1.11
	95.34	5.40	1.25	-	Bna	119.63	6.61	0.49	-	Cn	-	-	-	-	-	1.21
POM_C/10.0% HAp-g-PEG 2000	108.54	6.13	-	1.98	An	110.32	6.15	0.33	-	Fn	-	-	-	-	-	1.07
	109.57	5.66	0.68	-	Cn	124.47	7.30	-	2.02	An	-	-	-	-	-	1.08
	107.96	6.38	0.44	-	Bna	113.77	7.57	-	0.55	An	121.53	7.08	-	-	R2	1.10
POM_C/1.0% HAp-g-PEG 6000	110.31	6.42	0.90	-	Bna	93.29	4.02	1.28	-	Cn	-	-	-	-	-	1.00
	93.36	5.27	1.16	-	Bna	136.73	8.19	-	1.82	An	-	-	-	-	-	1.17
	126.38	7.44	-	1.51	An	77.93	2.36	1.47	-	Cn	-	-	-	-	-	1.24
POM_C/10.0% HAp-g-PEG 6000	119.72	7.21	0.52	-	Bna	129.27	6.62	-	2.19	An	-	-	-	-	-	1.00
	123.05	7.55	0.22	-	Bna	126.04	6.69	-	2.40	An	47.51	2.92	-	-	R3	1.04
	118.61	6.87	-	1.70	An	125.21	7.10	0.43	-	Fn	122.54	7.17	-	-	R3	1.05

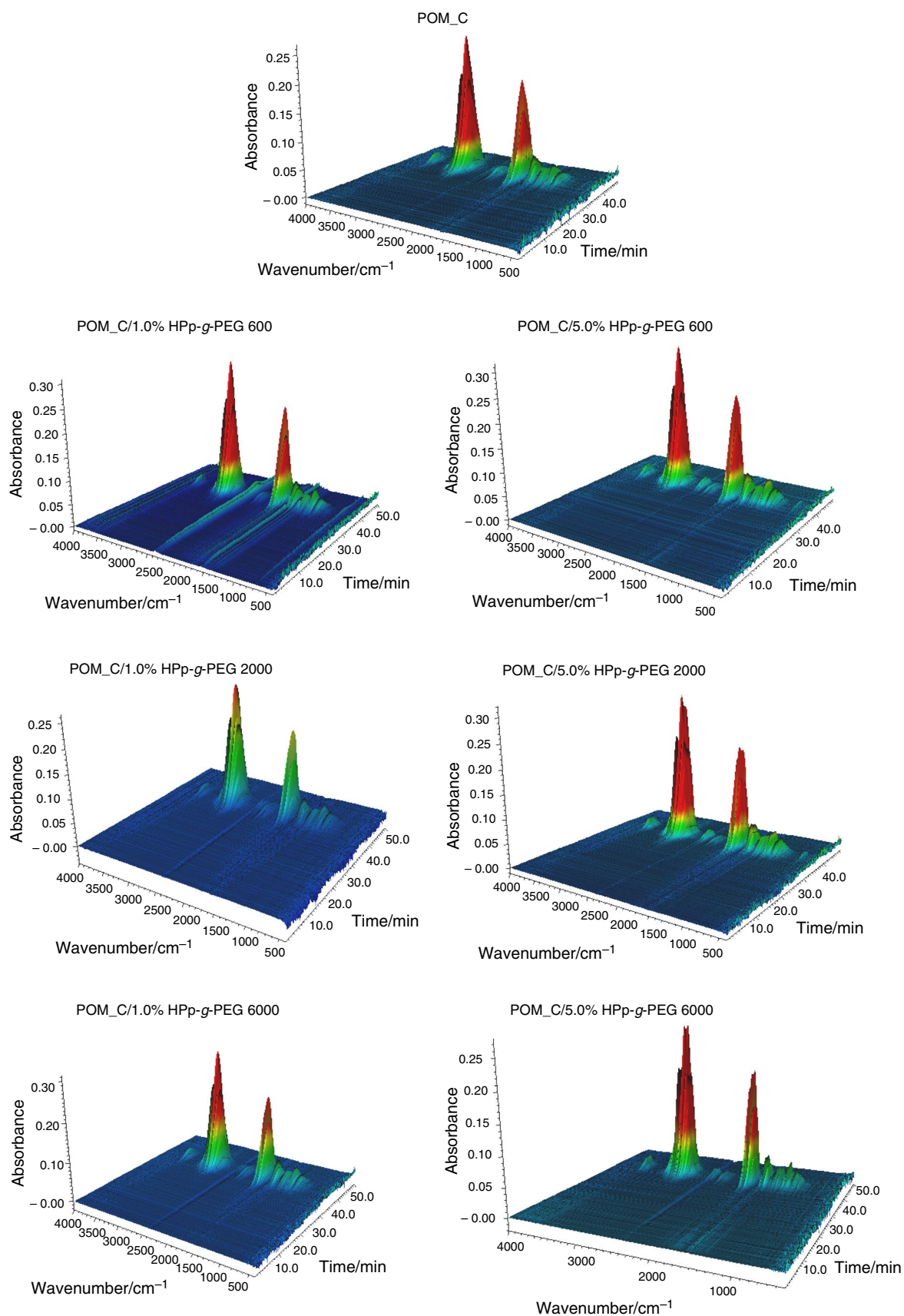
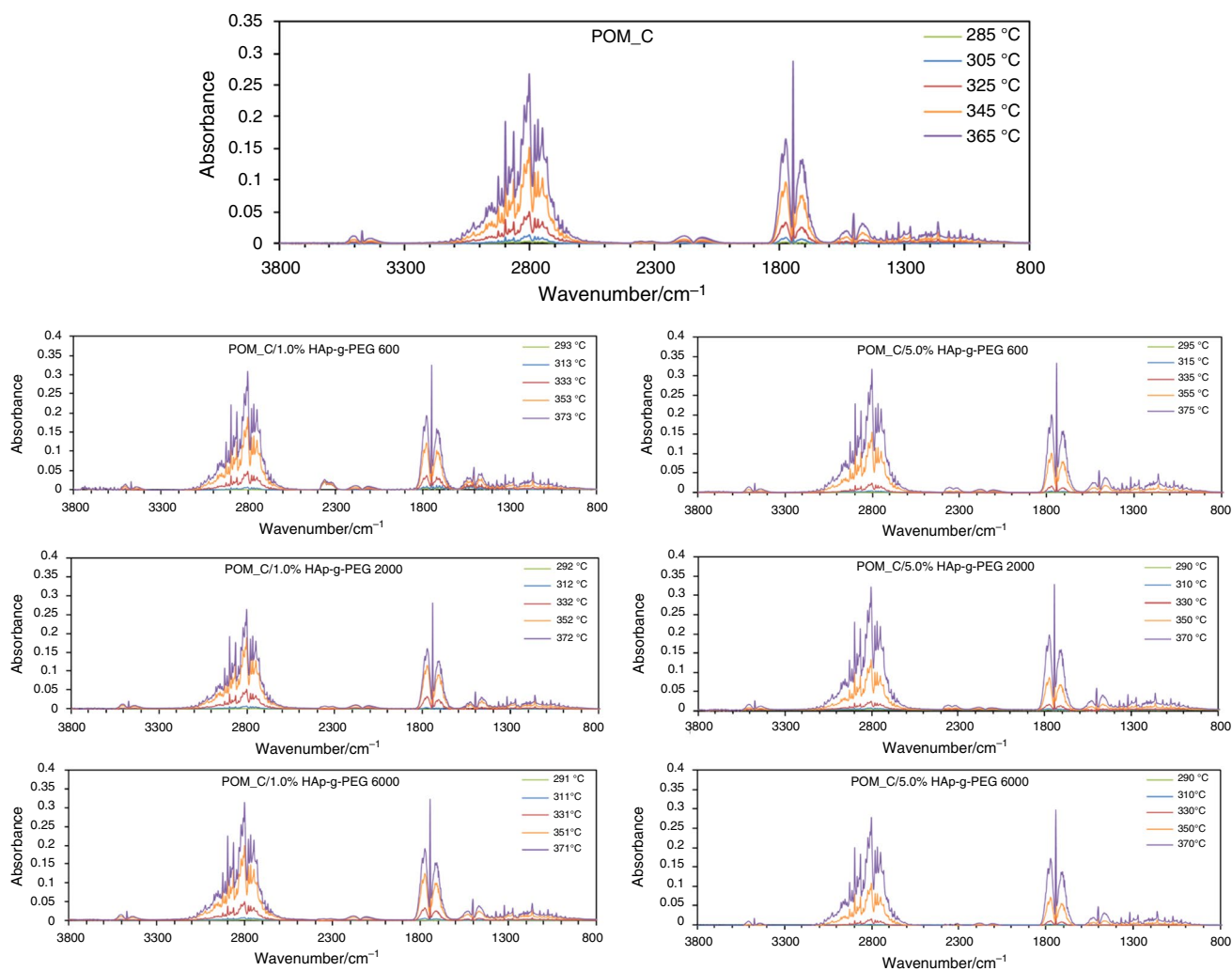


Fig. 5. 3D plots of IR spectra recorded during heating POM\_C and POM\_C composites with 1.0% and 5.0% HAp-g-PEG in the range from 25 to 550 °C



**Fig. 6** FTIR spectra of (i) POM\_C, and (ii) POM\_C composites with 1.0% and 5.0% HAp-g-PEG volatile decomposition products at selected decomposition temperatures

group of formaldehyde or carbon monoxide;  $1075\text{ cm}^{-1}$ ,  $1121\text{ cm}^{-1}$  and  $1165\text{ cm}^{-1}$  from the  $\nu\text{C-O}$  vibrations in esters and ethers;  $1744\text{ cm}^{-1}$  from vibrations  $\nu\text{C=O}$  in formaldehyde and  $2801\text{ cm}^{-1}$  from vibrations of  $\text{CH}_2$  groups in formaldehyde molecules [27]. The main decomposition product of POM\_C is formaldehyde, which is released from degrading polymer chains as a result of depolymerisation reactions from the chain ends and random chain breaking due to high temperature [7, 27]. Carbon monoxide and dioxide, methanol or ethanol, formic acid and methyl formate are released in much smaller amounts. In addition to formaldehyde, acidic compounds can also catalyse the decomposition of POM\_C. The spectra of composites containing 1.0% and 5.0% of HAp-g-PEG are very similar in shape to POM\_C. No band shifts or significant changes in their intensity were observed, which indicates a similar course of the POM\_C degradation reaction in these materials. Only a temperature shift is noted, which indicates a delay in the

POM\_C degradation reaction in the presence of the hybrid inorganic–organic additive.

The results of TG-MS analysis of selected volatile decomposition products of POM\_C and its composites with 1.0% and 5.0% HAp-g-PEG are presented in Fig. 7. The ion currents observed in the spectra come from fragments of the following compounds:  $m/z = 18$  ( $\text{H}_2\text{O}$ ),  $m/z = 29$  (fragment of formaldehyde molecule  $\text{H}_2\text{C=O}$ ),  $m/z = 30$  ( $\text{H}_2\text{C=O}$ ),  $m/z = 31$  (fragment  $-\text{CH}_3-\text{OH}$ ) and trioxane,  $m/z = 43$  ( $-\text{CH}_3-\text{COH}$ ),  $m/z = 44$  ( $\text{CO}_2$ ),  $m/z = 45$  (fragment of  $\text{HCOOH}$  and  $\text{CH}_3-\text{COOH}$ ),  $m/z = 46$  ( $\text{HCOOH}$ ),  $m/z = 57$  (fragment of additives used in POM),  $m/z = 60$  ( $\text{CH}_3-\text{COOH}$ ) and  $m/z = 61$  (phenyl groups derived from additives used in POM) [28].

The results obtained using mass spectrometry technique correspond well with the previous FTIR data, confirming the highest amount of formaldehyde formed during the thermal decomposition of pristine POM\_C. In addition to

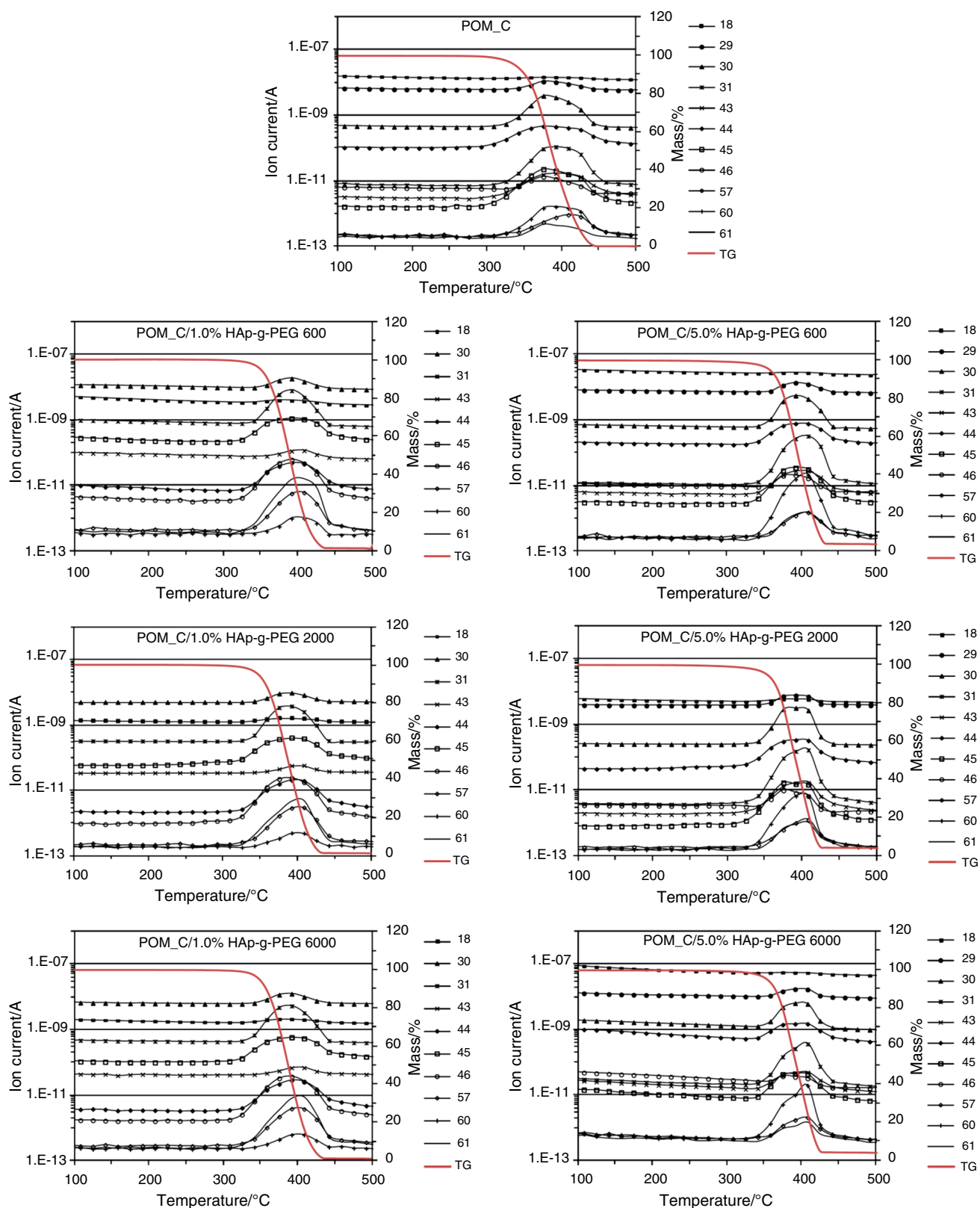


**Fig. 7** Results of TG-MS analysis: intensity of release of selected volatile decomposition products of POM\_C and POM\_C composites with 1.0% and 5.0% HAp-g-PEG

**Fig. 8** Heat release rate (HRR) profiles as a function of temperature and time for POM\_C and their composites with 5.0% and 10.0% HAp-g-PEG 600

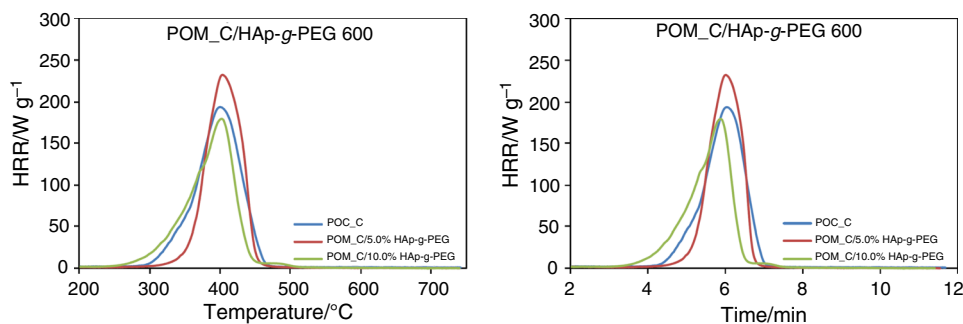


**Table 4** Flammability parameters determined from PCFC measurements: PHRR—maximum heat release rate, TTI—time to permanent ignition, THR—total heat released, and char residue

Material	PHRR/W g <sup>-1</sup>	PHRR/°C	PHRR/s	TTI/s	THR/kJ g <sup>-1</sup>	Residue/%
POM_C	191	402	361	254	14.2	0.00
POM_C/5.0% HAp-g-PEG 600	231	404	359	258	13.9	2.00
POM_C/10.0% HAp-g-PEG 600	178	402	352	194	12.8	8.18

formaldehyde, short products of POM\_C chain scission were recorded in a relatively large amount. Among the evolved gases were carbon dioxide; however, its concentration in the materials containing 1.0% HAp-g-PEG was significantly lower. At an even lower concentration, the presence of formic and acetic acid molecules was observed. In trace amounts, some compounds that were used as stabilizers for polyoxymethylene were detected. Unmodified POM\_C underwent almost complete thermal decomposition, while for composites containing 1.0% and 5.0% HAp-g-PEG addition, the char residue at 500 °C, consisting of mostly HAp, was 0.8–1% and 3.6–4%, respectively.

Among the POM-based composites, POM\_C/HAp-g-PEG 600 and POM\_H/HAp-g-PEG 600 were selected—based on the results of previous studies—for flammability tests. The aim of these investigations was to check whether the simultaneous improvement in the thermal stability of POM was accompanied by a reduction in the flammability of the tested composites. The measurements carried out using a PCFC microcalorimeter enabled to generate the heat release rate profiles (HRR [W g<sup>-1</sup>]) vs temperature and time, which are shown in Fig. 8. Based on the obtained profiles, the values of the flammability parameters, i.e. PHRR, TTI and THR, were determined, which are summarized in Table 4.

The HRR curves presented in Fig. 8 show that the combustion of POM and its composites is a violent process lasting about three minutes. The effect of HAp-g-PEG 600 incorporation on the POM combustion process is quite well visible. For POM\_C composite with 10.0% of HAp-g-PEG 600, the PHRR value decreased significantly. Moreover, it was found that the addition of HAp-g-PEG 600 had almost no effect on the temperature at which the maximum heat

release from the tested materials took place. There was a slight shift in time in the PHRR value, where for composites based on POM\_C there was a slight acceleration of combustion, which increased with an increasing amount of HAp-g-PEG 600. For 5.0% HAp-g-PEG 600 addition, no significant effect was observed on TTI, while 10.0% of the additive content led to a significant ignition acceleration for composites containing POM\_C. With the increase in the content of the additive in POM\_C composites there was a slight decrease in the THR value caused by a lower amount of polymer in composite materials at the expense of HAp, which is an inert component during the combustion process.

The last parameter was the percentage of solid residue after the combustion process. POM\_C was completely burned (solid residue 0%). In composites based on POM\_C, the solid residue was related to the HAp content in the HAp-g-PEG 600 additive used.

Due to the complexity of the HRR curves, they were deconvolved in order to separate overlapping peaks. The results are shown in Fig. 9.

For unmodified POM\_C, the HRR curve was composed of three peaks, the maxima of which were at the following temperatures: 346.7, 395 and 423.6 °C. The middle peak had the highest value, corresponding to a burning rate of 167.3 W g<sup>-1</sup>. The addition of HAp-g-PEG 600 to POM\_C resulted in the appearance of additional peaks on the HRR curve, the maxima of which were at the temperatures of 441.5 °C (for POM\_C/5.0% HAp-g-PEG 600) and 435.0 and 441.9 °C (for POM\_C/10.0% HAp-g-PEG 600), which corresponds most likely with the combustion of the organic part of the additive used.

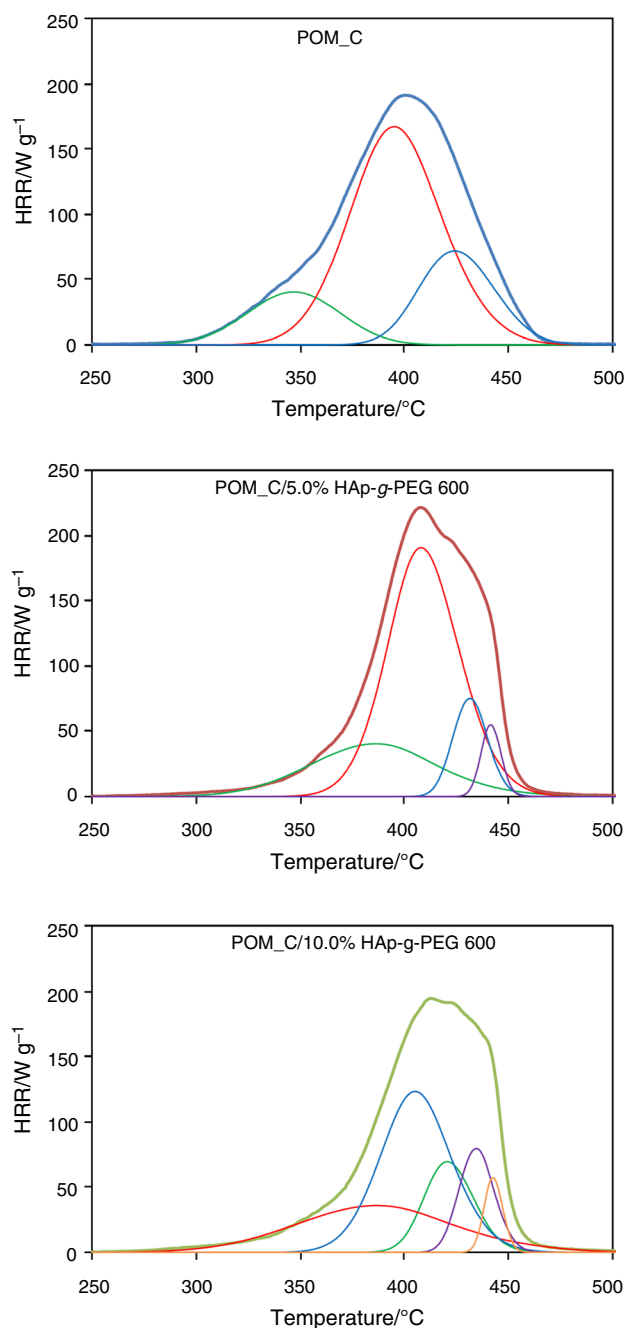


**Fig. 9** HRR curves after peak deconvolution for POM\_C and their composites with 5.0% and 10.0% HAp-g-PEG 600

**Table 5** UL 94 flammability classes horizontal test results for POM\_C and its composites with 1.0% and 5.0% HAp-g-PEG 600

Material	Burning time/s	Burning rate/mm s <sup>-1</sup>	Number of drops	Complete burn	Inflammation of the tissue paper	Charcoal	Flame
POM_C	189 ± 11	0.37 ± 0.02	109 ± 4	Yes	Yes	No	Yellow
POM_C/1.0% HAp-g-PEG 600	167 ± 17	0.42 ± 0.04	71 ± 8	Yes	Yes	No	Yellow–pink
POM_C/5.0% HAp-g-PEG 600	183 ± 27	0.39 ± 0.06	24 ± 3	Yes	Yes	Yes	Blue

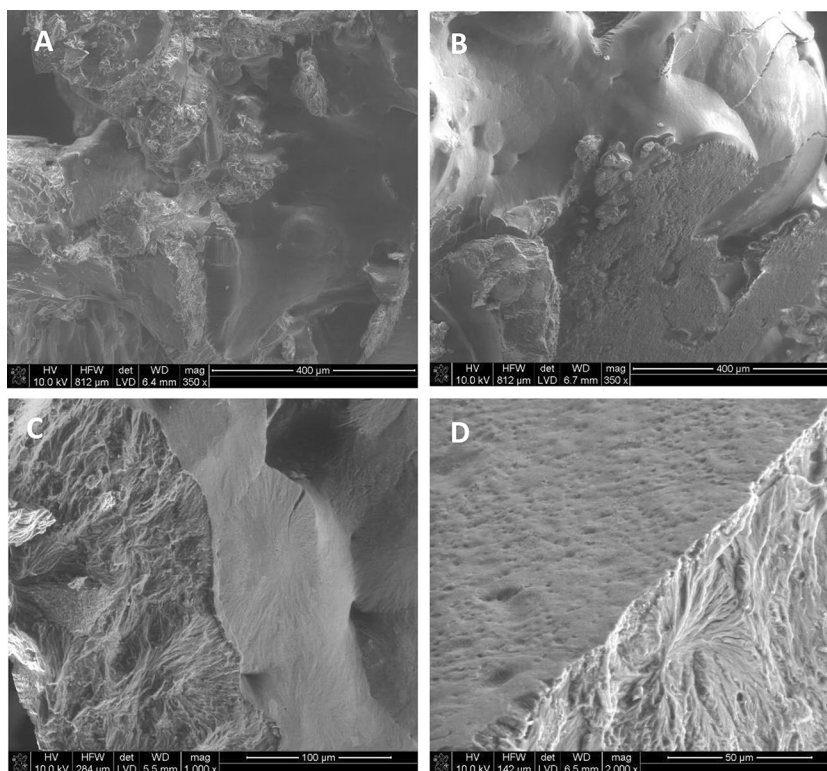
Next, horizontal burning test to determine the flammability class UL 94 HB. It is a method of determining the horizontal burning rate of a material after exposure to a small flame for a period of 15 s. The tests were carried out for POM\_C and its composites with 1.0% and 5.0% HAp-g-PEG 600, and the results are summarized in Table 5.

The measurements show that for low content of HAp-g-PEG (1.0%) in POM\_C-based composites, the combustion time is slightly shortened, while the combustion speed increases. At 5.0% of the additive content in the composites, the burning time and rate are comparable with the unmodified POM\_C. An important piece of information is the number of droplets falling during the combustion of the material, because dripping hot polymer can cause extensive burns to the skin, and the burning droplets cause further fire propagation, constituting an additional source of ignition [29, 30]. For the tested composite materials, with the increase in HAp-g-PEG 600 content, the amount of droplets falling during combustion was significantly reduced. For POM/HAp-g-PEG 600 (5.0%) composite, the combustion led to formation of char that limit the flow of oxygen to the burning sample, thus limiting the rate of its combustion. The colour of the flame that depends on the chemical composition of the combusted material changed with the material's composition from yellow (for pure POM\_C) through yellow-pink to blue (for POM\_C/5.0% HAp-g-PEG 600). In the sample of unmodified POM\_C, only C, H and O atoms are present, whereby in the composites, additionally N, Ca and P atoms occur, which may affect the colour of the flame during the combustion process [31, 32].

Morphology of char residue after combustion for samples POM\_C/1.0% HAp-g-PEG 600 and POM\_C/5.0% HAp-g-PEG 600 was presented in Fig. 10.

Morphology of char residue of POM\_C/1.0% HAp-g-PEG 600 after combustion shows a well-developed foam-like structure, whereby for POM\_C/5.0% HAp-g-PEG 600 there is a more dense microstructure which may indicate the reinforcement effect of HAp-based modifier at its higher load.

**Fig. 10** Morphology of char residue after combustion for samples POM\_C/1.0% HAp-g-PEG 600 (a, b) and POM\_C/5.0% HAp-g-PEG 600 (c, d)



## Conclusions

The obtained results show that incorporation of HAp-g-PEG to POM\_C leads to significantly improvement of the thermal stability of POM\_C, even by 32 °C, and the thermal decomposition parameters generally increase with higher HAp-g-PEG load. Noteworthy, the HAp-HDI-PEG 600 system turned out to be the most effective thermal stabilizer. Kinetic analysis of the degradation process of POM\_C/HAp-g-PEG composites shows that, in contrast to pure POM\_C, in which a one-stage decomposition takes place during heating as a result of first-order reactions with an accompanying autocatalytic effect (Bna, Cn), for systems containing the addition of HAp g-PEG thermal degradation is a more complex process. A small amount of this additive (1.0%) changes the kinetic scheme to the reaction (Bna, Cn) with simultaneous  $n$ -dimensional nuclei growth (An). With a higher amount of HAp-g-PEG filler (10.0%), decomposition occurs as a result of subsequent reactions in which no autocatalytic effect is observed ( $An \rightarrow Fn - n$ -th order reaction). The end of the degradation process is accompanied by reactions at the interface. As a result, the degradation process slows down and the thermal stability of the tested materials increases. The results of the TG-FTIR/MS method confirmed the increased stability of composites containing HAp-g-PEG compared to pure POM\_C, with the greatest improvement in thermal stability for materials containing 5.0% HAp-g-PEG 600. The main decomposition product for all analysed materials was

POM\_C-derived formaldehyde. Formic and acetic acid and small amounts of CO<sub>2</sub> were released to a much lesser extent. All of the above compounds are capable of further autocatalysis of the POM\_C degradation process, however, in the case of composites, this process was slowed down. Flammability testing with a PCFC microcalorimeter confirmed the high flammability of POM, including it as a highly flammable material (flammability class HB). Contrary to the improvement of the thermal stability of POM\_C, the addition of HAp-g-PEG 600 did not reduced the POM flammability. However, PHR, TTI and THR parameters for lower for POM\_C/10,0% HAp-g-PEG 600 composite as compared to unmodified polyoxymethylene.

The horizontal burning test for the UL 94 HB flammability class showed almost no effect of the addition of HAp-g-PEG 600 on the burning time and rate of the tested composites. However, there was a significant reduction in the amount of dripping from the material during the burning of droplets, which is a very important parameter from the point of view of fire spread.

**Acknowledgements** The authors are grateful to the Polish National Science Centre for financial support under the contract No. UMO-2016/21/B/ST8/00449. This work was supported by the subsidy of the Ministry of Education and Science for the AGH University of Science and Technology in Kraków (Project No 16.16.160.557).

**Open Access** This article is licensed under a Creative Commons Attribution 4.0 International License, which permits use, sharing,

adaptation, distribution and reproduction in any medium or format, as long as you give appropriate credit to the original author(s) and the source, provide a link to the Creative Commons licence, and indicate if changes were made. The images or other third party material in this article are included in the article's Creative Commons licence, unless indicated otherwise in a credit line to the material. If material is not included in the article's Creative Commons licence and your intended use is not permitted by statutory regulation or exceeds the permitted use, you will need to obtain permission directly from the copyright holder. To view a copy of this licence, visit <http://creativecommons.org/licenses/by/4.0/>.

## References

1. Archodoulaki VM, Luftl S, Seidler S. Degradation behavior of polyoxymethylene: influence of different stabilizer packages. *J Appl Polym Sci.* 2007;105:3679–88.
2. Zhou S, Wu Y, Zou H, Liang M, Chen Y. Tribological properties of PTFE fiber filled polyoxymethylene composites: the influence of fiber orientation. *Compos Commun.* 2021;28: 100918.
3. Saravanan ST, Kailasanathan C, Natarajan E, Ramasamy A. Crystallinity change and reduced warpages on thin walled parts-the effect of nano fumed silica on polyacetal. *SILICON.* 2021;13:4611–22.
4. Merijs Meri R, Zicans J, Ābele A, Ivanova T, Kalniņš M, Kundziņš K. Modification of polyoxymethylene for increased thermal resistance. *Polym Eng Sci.* 2017;57:772–8. <https://doi.org/10.1002/pen.24625>.
5. Lüftl S, Richaud E. Chemical Resistance of Polyoxymethylene. 2014. p. 23.
6. Polyacetals PK. In: Olabisi O, Adewale K, editors. *Handbook of thermoplastics.* Boca Raton: CRC Press; 2015. p. 193–249.
7. Luftl S, Archodoulaki VM, Seidler S. Thermal-oxidative induced degradation behaviour of polyoxymethylene (POM) copolymer detected by TGA/MS. *Polym Degrad Stab.* 2006;91:464–71.
8. Archodoulaki VM, Luftl S, Seidler S. Thermal degradation behaviour of poly(oxymethylene): 1. Degradation and stabilizer consumption. *Polym Degrad Stab.* 2004;86:75–83.
9. Archodoulaki VM, Luftl S, Seidler S. Oxidation induction time studies on the thermal degradation behaviour of polyoxymethylene. *Polym Test.* 2006;25:83–90.
10. Ohkatsu Y, Matsuura T, Yamato M. A phenolic antioxidant trapping both alkyl and peroxy radicals. *Polym Degrad Stab.* 2003;81:151–6.
11. Zhao XW, Ye L, Li HL. Study on the high efficiency antioxidant of polyoxymethylene. *Polym Plast Technol Eng.* 2006;45:1181–90.
12. Hu Y, Ye L. Study on the thermal stabilization effect of polyamide on polyoxymethylene. *Polym Plast Technol Eng.* 2006;45:839–44.
13. Sun T, Ye L, Zhao X. The thermostabilization of polyoxymethylene through amine treatment. *Polym Plast Technol Eng.* 2008;47:404–10.
14. Shi J, Jing B, Zou X, Luo H, Dai W. Investigation on thermostabilization effect and nonisothermal degradation kinetics of the new compound additives on polyoxymethylene. *J Mater Sci.* 2009;44:1251–7.
15. Archodoulaki V-M, Lüftl S, Seidler S. Thermal degradation behaviour of poly(oxymethylene): 1. Degradation and stabilizer consumption. *Polym Degrad Stab.* 2004;86:75–83.
16. Wypych G. POM polyoxymethylene. In: Wypych G, editor. *Handbook of polymers.* 2nd ed. ChemTec Publishing; 2016. p. 490–6.
17. Whelan T. *Polymer technology dictionary.* London: Chapman & Hall; 1994.
18. Sun S, He Y, Wang X, Wu D. Flammability characteristics and performance of halogen-free flame-retarded polyoxymethylene based on phosphorus–nitrogen synergistic effects. *J Appl Polym Sci.* 2010;118:611–22. <https://doi.org/10.1002/app.32465>.
19. Pielichowska K, Szczygielska A, Spasówka E. Preparation and characterization of polyoxymethylene-copolymer/hydroxyapatite nanocomposites for long-term bone implants. *Polym Adv Technol.* 2012;23:1141–50. <https://doi.org/10.1002/pat.2012>.
20. Król-Morkisz K, Karaś E, Majka TM, Pielichowski K, Pielichowska K. Thermal stabilization of polyoxymethylene by PEG-functionalized hydroxyapatite: examining the effects of reduced formaldehyde release and enhanced bioactivity. *Adv Polym Technol.* 2019. <https://doi.org/10.1155/2019/9728637>.
21. Pielichowska K, Król K, Majka TM. Polyoxymethylene-copolymer based composites with PEG-grafted hydroxyapatite with improved thermal stability. *Thermochimica Acta.* 2016;633.
22. Pielichowska K. Thermooxidative degradation of polyoxymethylene homo- and copolymer nanocomposites with hydroxyapatite: kinetic and thermoanalytical study. *Thermochim Acta.* 2015;600:7–19.
23. Lüftl S, Richaud E. Chemical resistance of polyoxymethylene. *Polyoxymethylene handbook.* Hoboken: John Wiley & Sons, Inc.; 2014. p. 277–99. <https://doi.org/10.1002/9781118914458.ch11>.
24. Pielichowski K, Njuguna J, Limited RT. *Thermal degradation of polymeric materials.* Rapra Technology; 2005.
25. Zhou D, Porter W, Zhang G. Drug stability and degradation studies. In: *Developing solid oral dosage forms.* 2009. p. 87–124.
26. Grassie N, Roche R. The thermal degradation of polyoxymethylene. *Die Makromolekulare Chemie.* 2003;112:16–33.
27. Duan Y, Li H, Ye L, Liu X. Study on the thermal degradation of polyoxymethylene thermogravimetry-Fourier transform infrared spectroscopy (TG-FTIR). *J Appl Polym Sci.* 2006;99:3085–92.
28. Lüftl S, Archodoulaki V-M, Seidler S. Thermal-oxidative induced degradation behaviour of polyoxymethylene (POM) copolymer detected by TGA/MS. *Polym Degrad Stab.* 2006;91:464–71.
29. Matzen M, Kandola B, Huth C, Schartel B. Influence of flame retardants on the melt dripping behaviour of thermoplastic polymers. *Materials.* 2015;8:5621–46.
30. Iwko J. Zachowanie się tworzyw sztucznych w warunkach pożarowych. 2. pomiary palności oraz metody uniepalniania tworzyw sztucznych. *Tworzywa sztuczne i chemia.* 2009;6:24.
31. Zhang J, Shields TJ, Silcock GWH. Effect of melting behaviour on upward flame spread of thermoplastics. *Fire Mater.* 1997;21:1–6.
32. Wang Z-Y, Liu Y, Wang Q. Flame retardant polyoxymethylene with aluminium hydroxide/melamine/novolac resin synergistic system. *Polym Degrad Stab.* 2010;95:945–54.

**Publisher's Note** Springer Nature remains neutral with regard to jurisdictional claims in published maps and institutional affiliations.